JOURNAL OF MATERIALS SCIENCE 23 (1988) 2121–2128

Mechanical testing of plasma-sprayed coatings of ceramics

C. COLIN, M. BOUSSUGE, D. VALENTIN
Ecole Nationale Supérieure des Mines de Paris, Centre des Matériaux, BP 87, 91003 Evry Cédex, France

G. DESPLANCHES
Régie Nationale des Usines Renault, Direction des Laboratoires Automobiles, 92109 Boulogne Billancourt Cédex, France

Mechanical tests have been performed on two types of plasma-sprayed ceramic coatings: magnesium zirconate (ZM) on aluminium alloy and chromium oxide (CO) on cast iron. Tensile strength, shear strength, energy relaxation rate and crack velocity have been determined. Results obtained with double-torsion tests show good agreement with those of double-cantilever-beam tests. Fracture always occurred in the ceramic for the ZM coating and at the interface for the CO one. Finally, acoustic emission monitoring carried out during bending tests was used to point out different types of emission, and to correlate them with micrographic examinations in order to identify some damaging processes.

1. Introduction

For diesel engines as well as for gas turbines, plasma-spraying of ceramics appears to be an interesting alternative to the use of monolithic components, for which the problem of the fixture to metallic parts has yet to be solved. However, a performant coating should exhibit strong adhesion with the substrate and good intrinsic mechanical properties. Moreover, reproducibility of the layer can only be obtained through severe control of the powder, the surface preparation and the spraying conditions: specific methods of testing should be developed, in order to evaluate the quality of the coatings.

This paper summarizes some mechanical tests per formed on ceramic coatings plasma-sprayed on metallic substrates. It compares and discusses some experimental methods and the results obtained for two different types of coating.

2. Materials

The materials considered in this study are representative examples of the two principal applications of ceramic coatings in diesel engines: a magnesium zirconate (ZM) used as a thermal barrier, and chromium oxide (CO) used for wear resistance improvement. Both coatings have been made with the self-acting plasma torch equipment of the Regie Nationale des Usines Renault, which offers maximal guarantee of reproducibility. The principal characteristics of the coatings and substrates are summarized in Table I.

3. Tensile and shear strength measurements

Following the method used by several authors [1–3], specimens were made by joining with an epoxy glue, as shown in Fig. 1. A specific device was used to prevent misalignment. The dimensions of the whole specimen (10 mm × 10 mm × 160 mm) allowed a surface of 100 mm^2 of coating to be tested. The two different types of loading applied to these specimens to evaluate tensile and shear strengths of the layer are illustrated schematically in Fig. 1.

During tensile tests, fracture occurred systematically at the metal–ceramic interface for the CO coating (adhesive fracture), and more often than not in the ceramic layer for the ZM coating (cohesive fracture). The mean rupture strengths (the standard error is given in brackets) measured on 10 specimens were, respectively,

$$\sigma_{fCO} = 26.1\ (3.3)\ \text{MPa} \qquad \sigma_{fZM} = 12.7\ (2.1)\ \text{MPa}$$

In the shear tests, the coating was situated close to the outer loading point, in order to minimize the effects of the bending moment. Moreover, the prints of the loading points on the broken specimens permitted verification that there was no evident correlation between the measured strength and the position of the coating with regard to the applied load.

Fractographic examination showed that 7 out of 20 specimens failed partially or totally in the epoxy layer or between the epoxy and the ceramic. Moreover, interfacial fracture was always observed for the CO, while ZM coatings presented a bevelled fracture surface, probably due to the influence of normal stresses. Assuming the shear stress is constant throughout the section, the mean shear strength values obtained for significant ruptures were

$$\tau_{fCO} = 20.2\ (5.2)\ \text{MPa} \qquad \tau_{fZM} = 10.3\ (2.1)\ \text{MPa}$$

4. Fracture energy measurements

To the authors' knowledge, only two types of test

0022–2461/88 $03.00 + .12

TABLE I Principal properties of the materials studied

Property	Coating	
	ZM on Aluminium alloy	CO on cast iron
Coating		
Powder composition (wt %)	ZrO_2–MgO (76:24)	Cr_2O_3
Porosity (%)	5 to 8	8
Thickness (mm)	1.5	0.3
Young's modulus (GPa)	65	120
Thermal expansion coefficient $(°C)^{-1}$	10.7×10^{-6}	7.1×10^{-6}
Intermediate layer		
Powder composition (wt %)	Progressive from Ni–Al (95:5) to ZrO_2–MgO (76:24)	–
Thickness (mm)	0.5	–
Substrate		
Composition (wt %)	Al + Si–Cu–Mg–Ni (12:1:1:1)	Fe + C–Si (3.4:2.1)
Young's modulus (GPa)	76	130
Elastic limit (MPa)	210	280
Fracture strength (MPa)	300	280
Thermal expansion coefficient $(°C)^{-1}$	23×10^{-6}	9.7×10^{-6}

have been used to characterize the fracture mechanics of ceramic–metal assemblies: double cantilever beam (DCB) [1, 4] and single edge notch beam (SENB) [2, 5, 6]. One aim of this work was to compare results obtained using a DCB specimen and a double-torsion (DT) specimen, the latter of which is easier to produce and offers a stress intensity factor K_I independent of the crack length a, but exhibits a complex curvilinear crack front.

All specimens were made by gluing; their dimensions are given in Fig. 2. The crack initiation was facilitated using a chevron-notch in ZM coatings, whereas the thinner CO layer was precracked with a Vickers indentation.

Initially, it was necessary to evaluate the influence of the heterogeneity of the specimens on the compliance calibration curves. As the Young's moduli of the ceramic layers were not very different to those of the substrates, our work was limited to checking that the very weakest epoxy layer did not significantly affect the compliance C of the specimens. With this objective, the compliances measured on metal–epoxy–metal DCB specimens were compared to those recommended by ASTM standards [7] for metals, the crack being simulated by a notch. The results obtained for aluminium alloy and cast-iron showed that the enhancement of the compliance induced by the glue remained very limited.

The DCB tests were performed using the conventional loading/unloading method, increasing the maximum load, which allowed the crack propagation to be monitored from the compliance variations. From time to time, the length of the crack was optically verified using a microscope.

In order to show up any slow crack growth, the crosshead of the test machine was stopped every time the maximum deformation was reached for a few minutes, during which the load evolution was observed. For the ZM coating as well as for the CO one, no significant subcritical crack growth occurred: the load plateau rapidly obtained during the relaxation always remained very close to the load to which the elastic loading curve deviated.

The successive values of the crack-arrest loads P

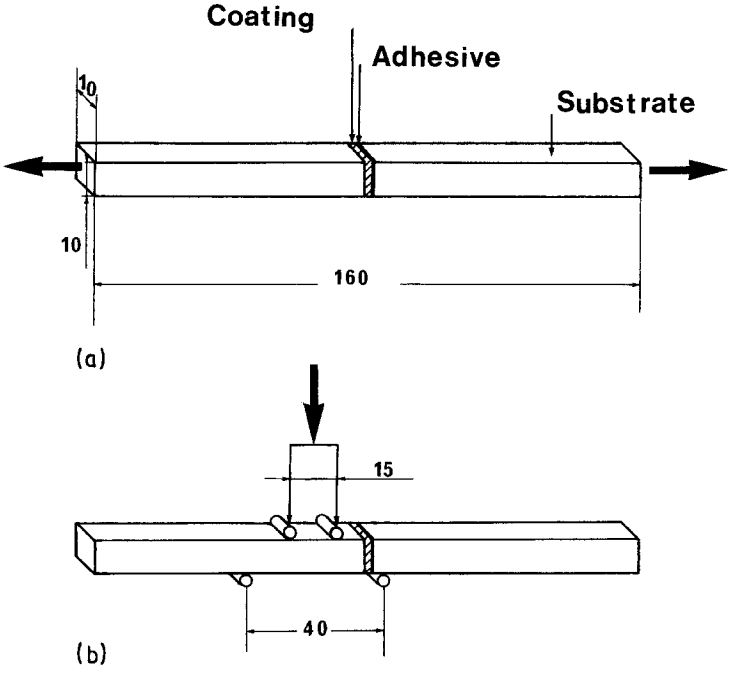

Figure 1 Method used for making and testing strength measurement specimens: (a) tensile strength, (b) shear strength. Dimensions in millimetres.

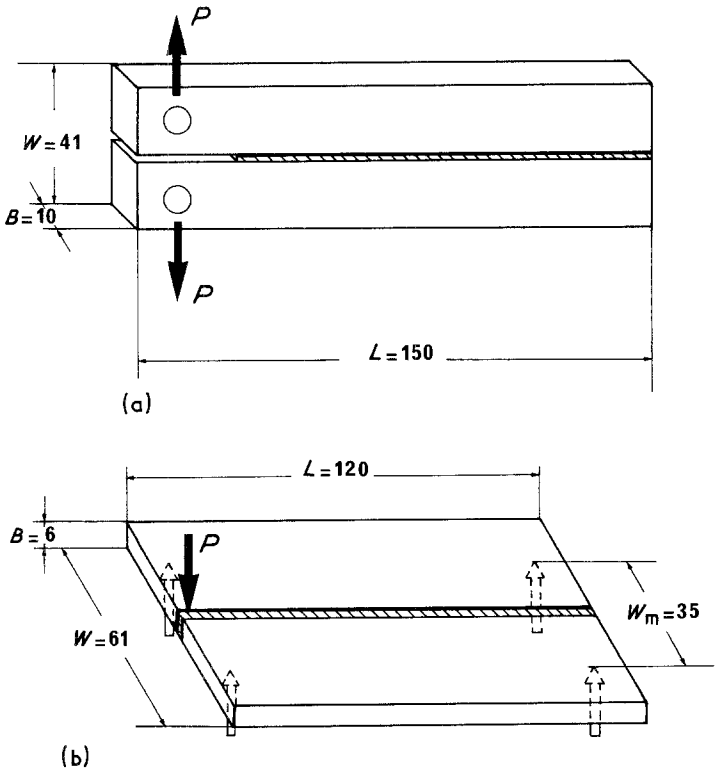

Figure 2 Specimens used for fracture energy measurements: (a) double cantilever beam, (b) double torsion. Dimensions in millimetres.

during relaxation allowed the R-curve to be determined using the expression giving the energy release rate:

$$G_I = \frac{P^2}{2B}\frac{dC}{da}$$

where B is defined in Fig. 2. The results obtained are gathered together in Fig. 3. They show that the energy release rate remains approximately constant during crack propagation. The average values (the standard error is given in brackets) of the energy release rates of the CO and of the ZM are, respectively,

$$G_{ICCO} = 96.3\ (7.0)\ J\,m^{-2}$$

$$G_{ICZM} = 59.8\ (3.2)\ J\,m^{-2}$$

According to the strength measurements, ZM presented a cohesive fracture, whereas CO exhibited an adhesive one.

Significant results of DT tests could only be obtained in the ZM coating because fracture always occurred, in spite of the precracking, at the glue–coating interface for CO. Relaxation tests were performed

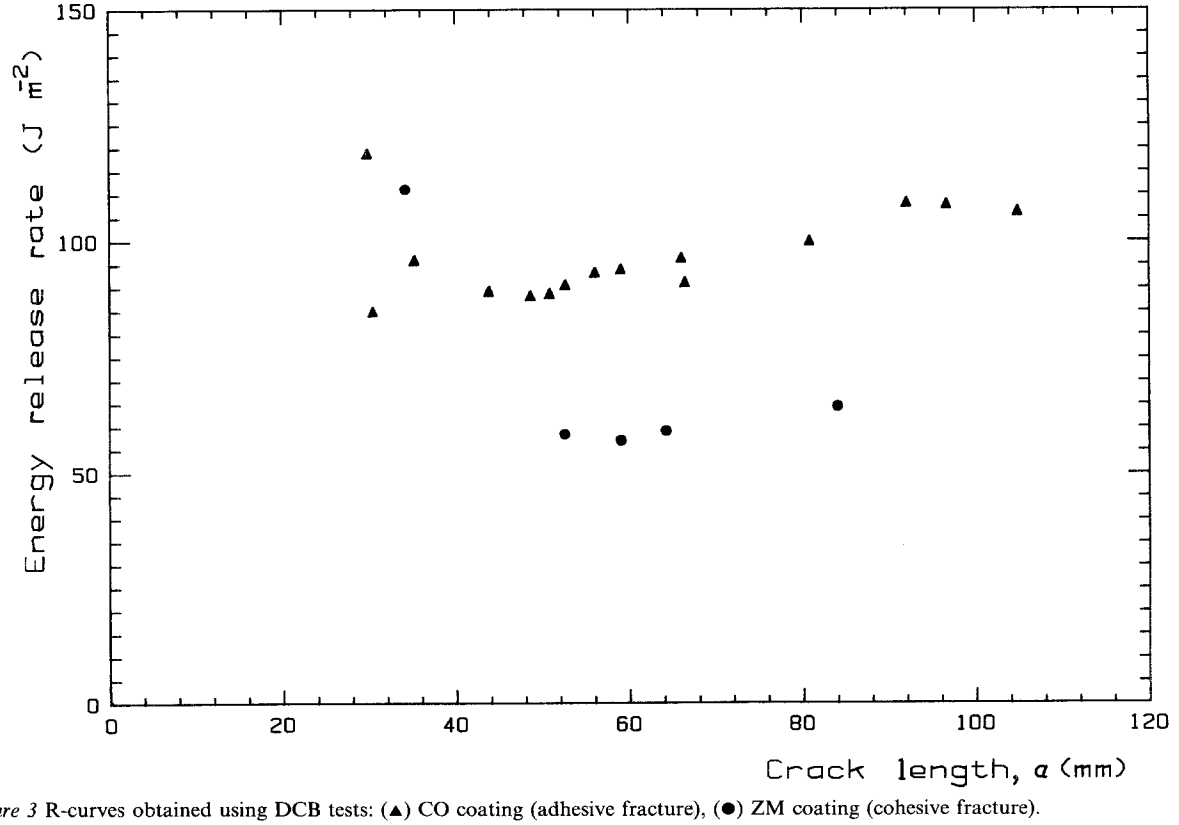

Figure 3 R-curves obtained using DCB tests: (▲) CO coating (adhesive fracture), (●) ZM coating (cohesive fracture).

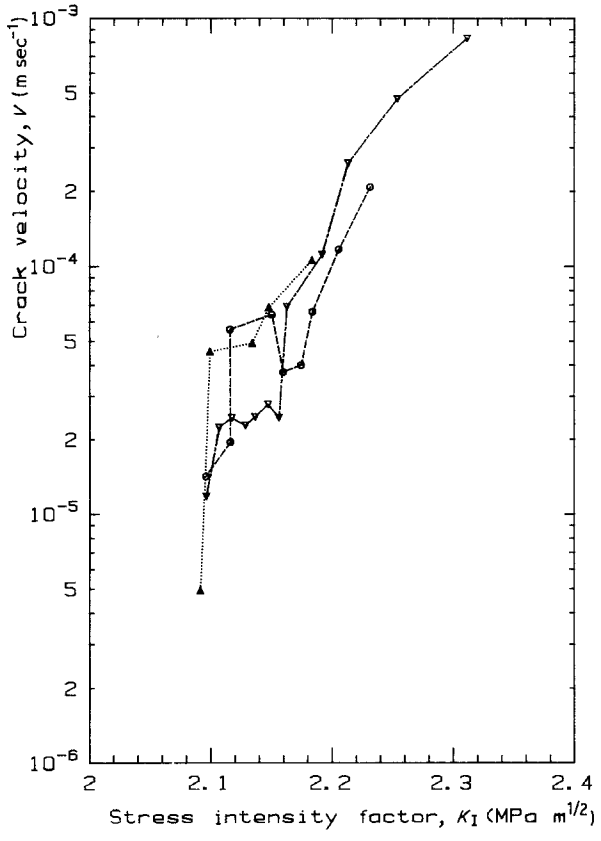

Figure 4 K_I–V diagram obtained on ZM coating using DT tests. $V = AK_I^n$ where $n = 60$, $A = 2.37 \times 10^{-24}$.

and hence allowed the average energy release rate (the standard error is given in brackets) to be determined, using the expression previously given for DCB tests:

$$G_{IC\,ZM} = 61.3\ (2.8)\ \mathrm{J\,m^{-2}}$$

The diagram giving the crack velocity $V = da/dt$ as a function of the stress intensity factor for the coating was also calculated, assuming a constant deflection y and a plane stress state with the expressions

$$K_I = P\left(\frac{E}{2B}\frac{dC}{da}\right)^{1/2} \qquad V = -\frac{y}{P^2}\left(\frac{dC}{da}\right)^{-1}\frac{dP}{dt}$$

in which the factor dC/da has been determined using an equation which considers the deformation of the uncracked part of the specimen [8]. This diagram, represented in Fig. 4, confirms the low sensitivity to subcritical crack growth: the crack velocity decreases very rapidly with decreasing stress intensity factor, with an average exponent of 60.

All these DT results are in good agreement with those obtained using DCB tests. With respect to the amount of data, they give proof of the capacity of the DT tests for the study of the fracture mechanics of plasma-sprayed coatings of ceramics. However, they show the limits of the method of gluing, particularly for the smooth surfaces of coatings destined for a wearing use: special care should be taken in choosing the glue and preparing the surface.

5. Acoustic emission during four-point bending tests

Acoustic emission (AE) monitoring was performed using a Series 3000 Dunegan equipment, associated with a PZT transducer Type S 1000 BM with a dominant frequency of 200 kHz. The system consisted of a 40 dB preamplifier with a frequency range of 100 to 300 kHz, an amplifier with an adjustable gain fixed at 50 dB, and an impulse detector transforming all peaks exceeding the threshold (25 dB) at the output into digital pulses (counts). The dB measurements were given with reference to a 1 μV signal at the transducer. The dead time of the analysis device was set to count one AE event for each series of pulses separated by less than 100 μsec.

Bending tests were performed with an outer span of

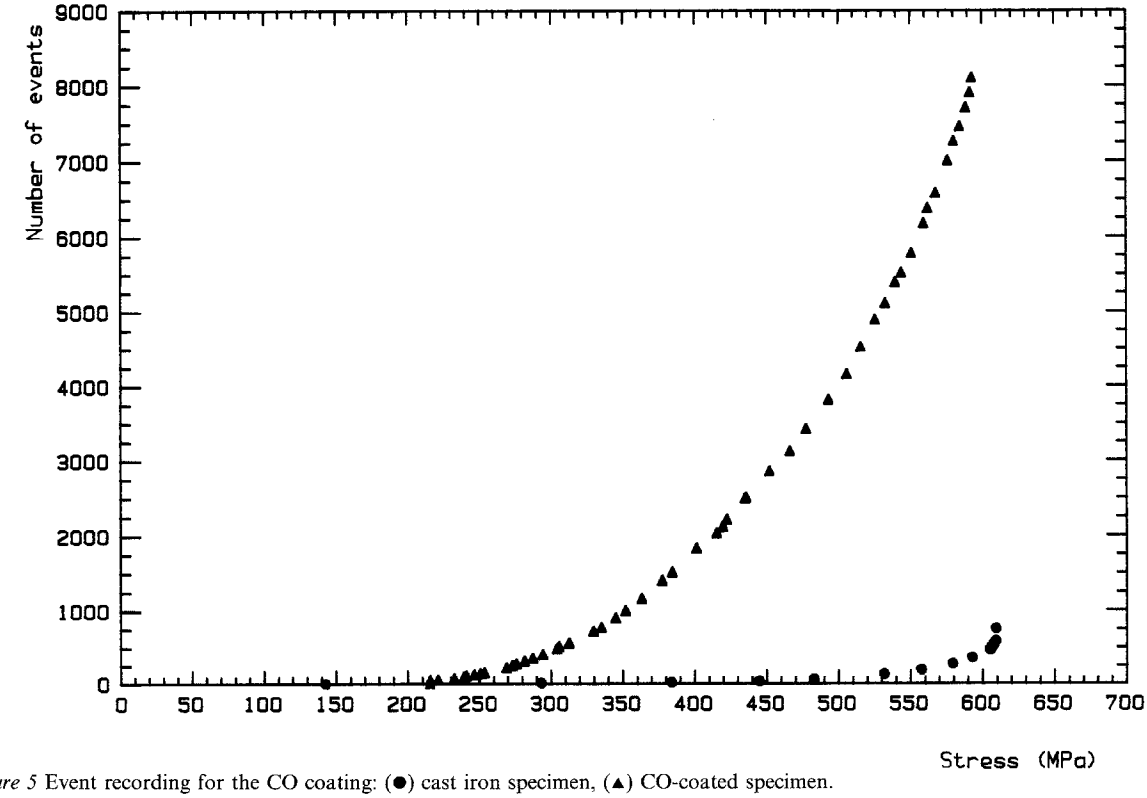

Figure 5 Event recording for the CO coating: (●) cast iron specimen, (▲) CO-coated specimen.

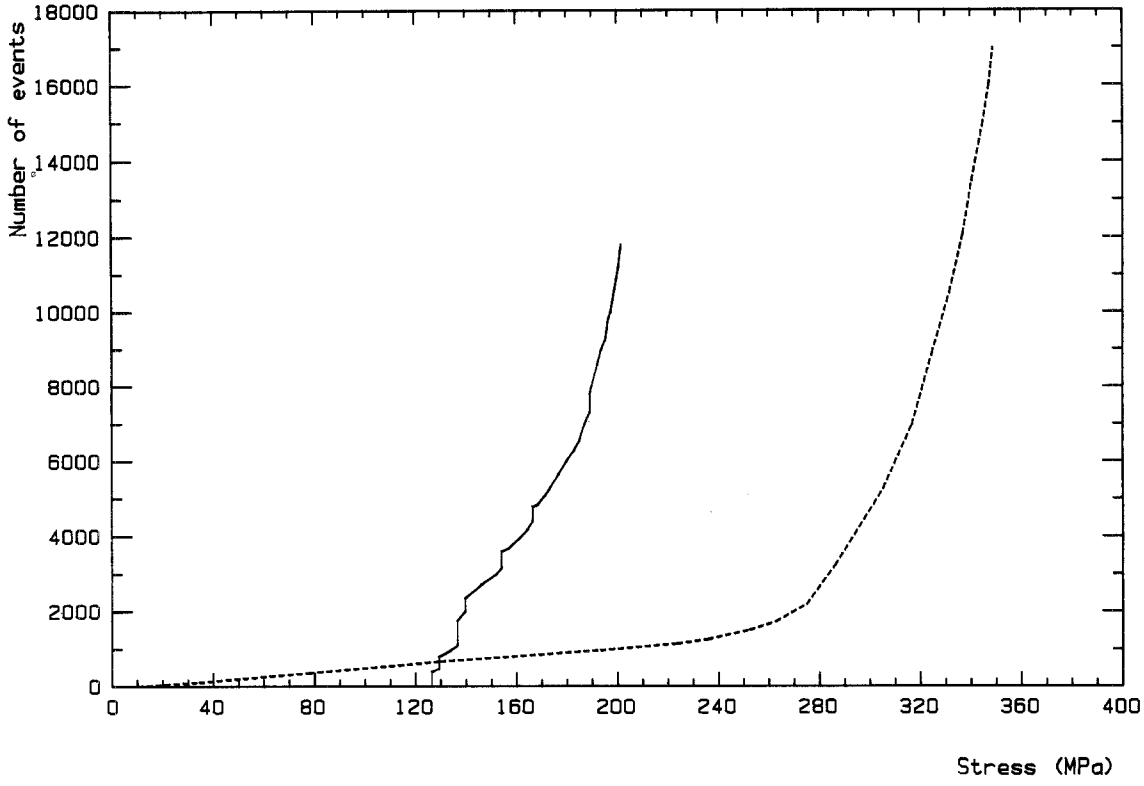

Figure 6 Event recording for the ZM coating: (– – –) aluminium alloy specimen, (——) ZM-coated specimen.

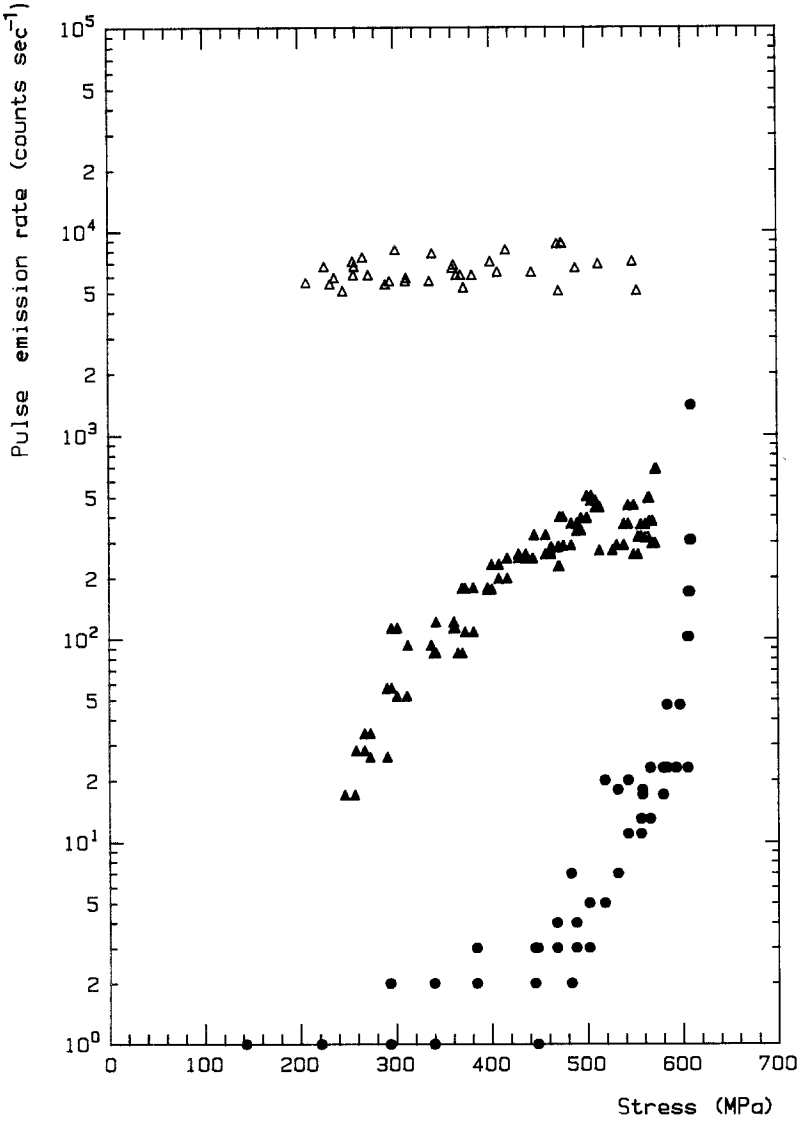

Figure 7 Pulse emission rate against applied stress for the CO coating: (●) cast iron specimen (▲) CO-coated specimen (low-rate AE), (△) CO-coated specimen (high-rate AE).

70 mm and an inner span of 15 mm, the dimensions of specimens being 10 mm × 10 mm × 80 mm. The coating, situated on the side in tension, was previously removed under the loading points to avoid AE by crushing. During the experiments, event and pulse count rates and maximum amplitude were recorded, in order to detect the damaging of the coating, and to identify the different crack growth processes.

The number of events as a function of the applied stress, represented in Figs 5 and 6, shows different behaviour for the two kinds of coating: the AE from the CO coating is more continuous than that obtained from the ZM one. For the latter type of specimen, the creation of a crack generated a step (about 500 events), whereas the CO coating failed in only one process (1 event). Relating to this observation, the monitoring of the damaging process of the CO coating was more successful in plotting the number of pulses as a function of the load, since the curve exhibited steps associated with crack creation.

The different thicknesses, and a crack propagation in ZM slower than in CO (possibly owing to a toughening mechanism), can explain the difference between the behaviours of the two coatings.

Figs 7 and 8 represent the pulse emission rates against the applied stress calculated using elastic and homogeneous assumptions, for coated specimens and for the associated uncoated substrates tested under the same conditions.

The number of peaks of high rate shows a good correlation with the number of cracks observed on the surface of the coating for both materials: this discrete AE at constant pulse count rate is generated by the Mode I cracking of the coatings.

The second type of AE was characterized by a lower pulse count rate increasing with the load, which always appeared after the first crack. Compared with the AE of a substrate alone, this one begins to operate in a range of loading in which metals exhibit no significant activity. Moreover, in the case of the ZM-coated aluminium alloy, the count rate is dependent on the deformation rate, which is characteristic of any viscoplastic behaviour.

On one hand, concerning the CO coating on cast-iron, this low-energy AE can be explained by optical microscopy examinations as shown in Fig. 9: in addition to the main emerging cracks, interfacial cracking (Mode II) and crack branching (mixed Modes I + II) occurred in the coating. Finally, some small cracks started from the interface, probably initiated at interfacial flaws. All these secondary cracks may be responsible for the low-energy AE.

On the other hand, Fig. 10 represents typical micrographs of the ZM coating: they show a main crack

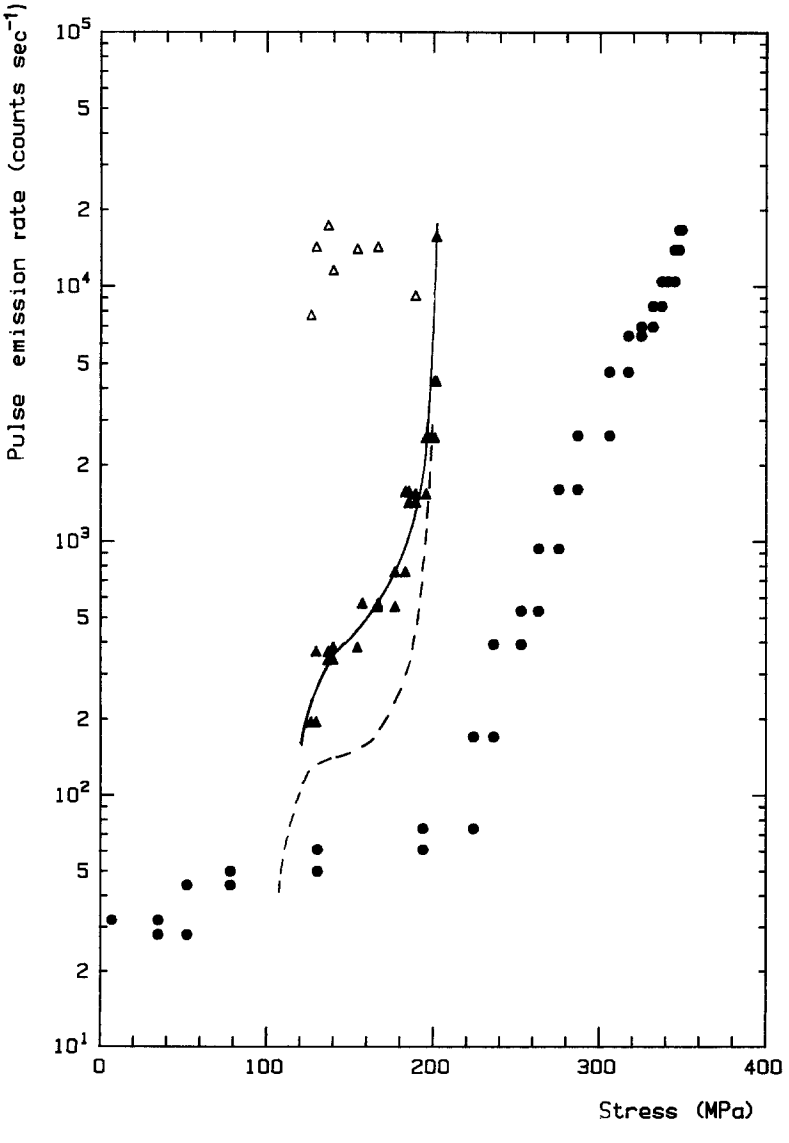

Figure 8 Pulse emission rate against applied stress for the ZM coating: (●) aluminium alloy specimen, (▲) ZM-coated specimens (low-rate AE), (△) ZM-coated specimen (high-rate AE). Crosshead speed (– – –) 0.05 mm min^{-1}, (——) 0.1 mm min^{-1}.

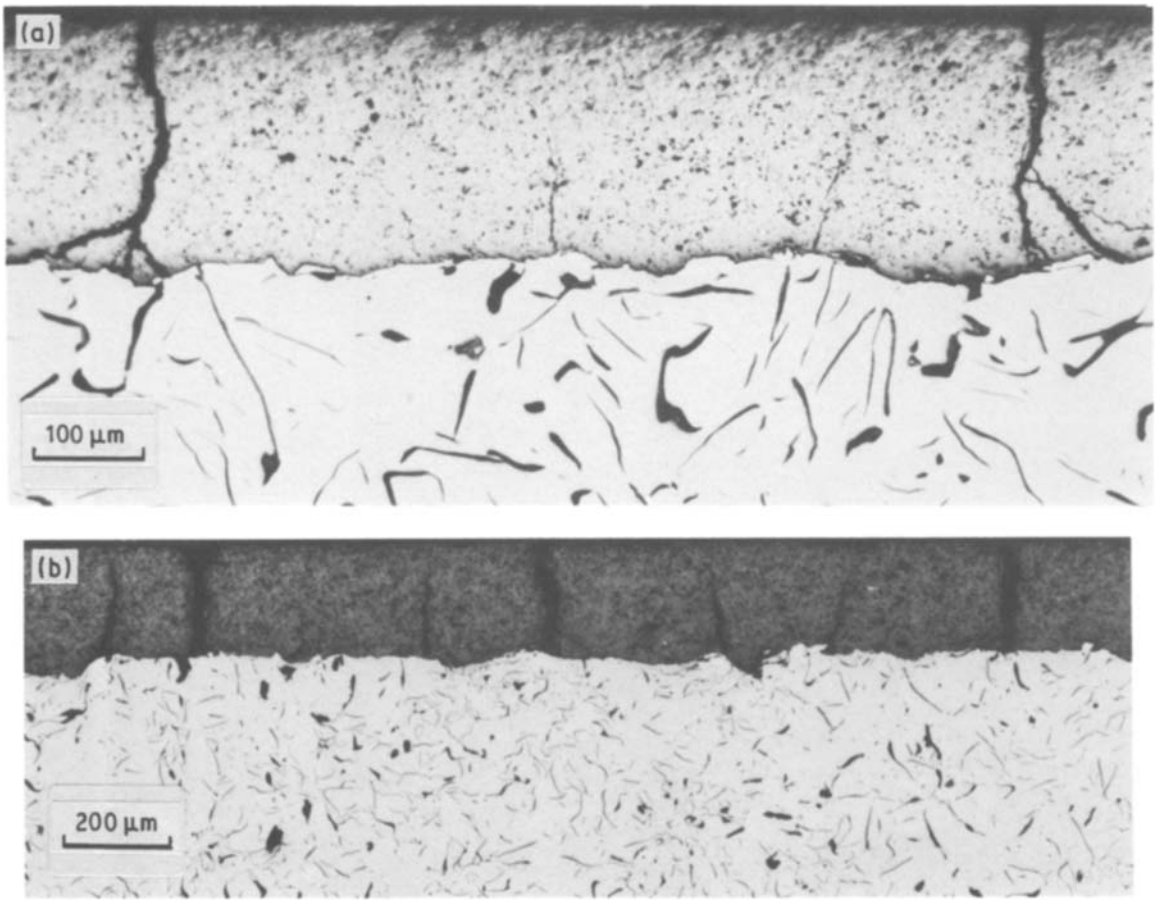

Figure 9 (a, b) Micrographs of cracked CO coating.

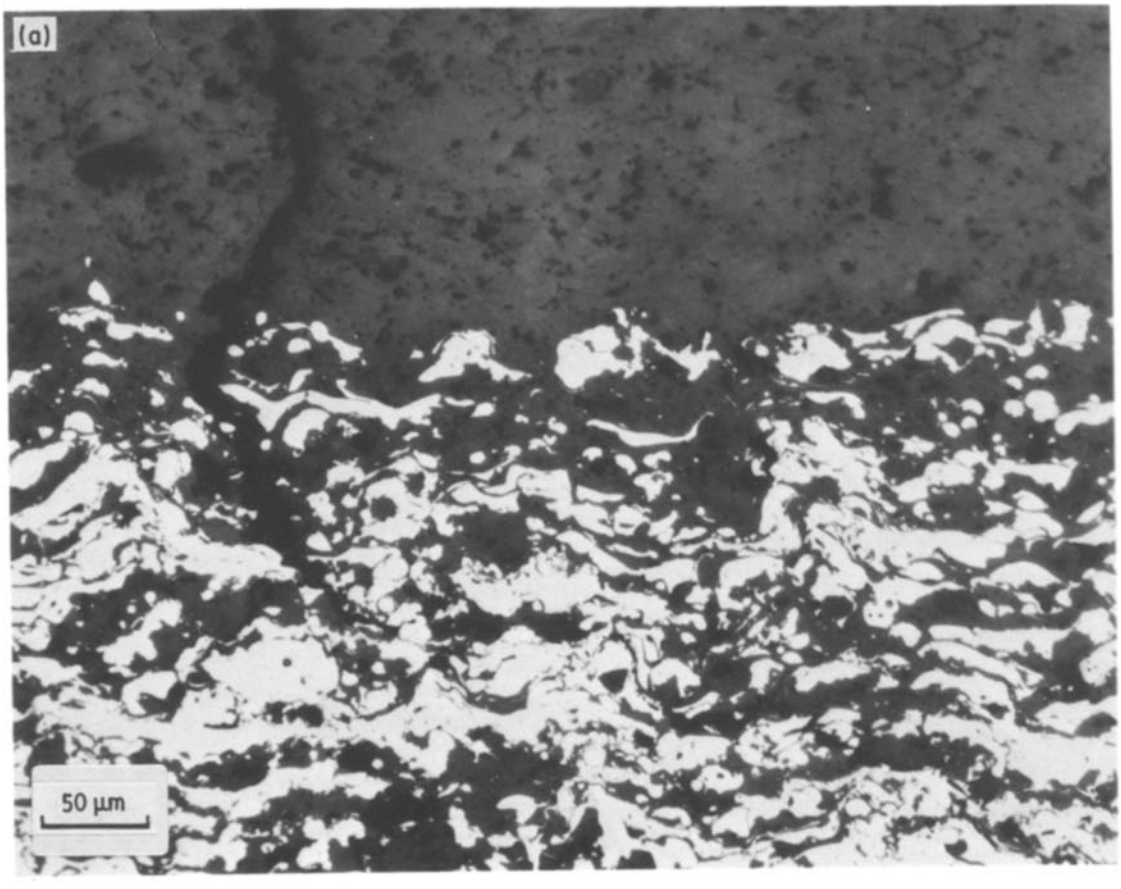

Figure 10 (a, b) Micrographs of cracked ZM coating.

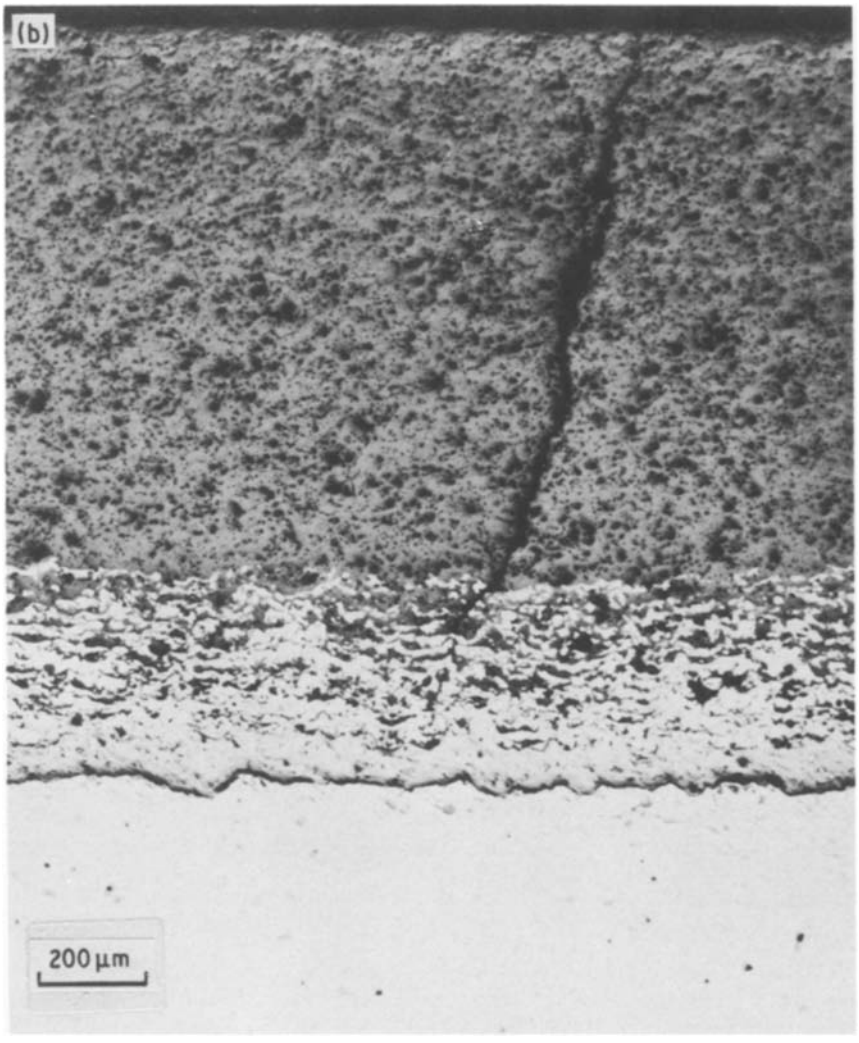

Figure 10 Continued.

passing round the first particles of Ni–Al alloy without obvious auxiliary cracking. Other damaging processes such as microcracking could however be involved, and hence be the cause of the AE. Moreover, the strength of the coated specimens is much lower than those of the metallic ones. This weakening of the substrate may be attributed to the coating process and/or to stress concentration effects affecting the substrate. Under this assumption, a localized plastification of the metal could also be the origin of a low-rate AE, and could explain the deformation rate dependence. Other tests would be necessary to verify this point.

6. Conclusion

The mechanical tests conducted on plasma-sprayed ceramic coatings on metallic substrates allowed the feasibility of some tests to be assessed, in order to obtain numerical values of the fracture strength and of the fracture energy of the coating. The tensile and shear strengths measured are, respectively, 26.1 and 20.2 MPa for chromium oxide (CO) and 12.7 and 10.3 MPa for magnesium zirconate (ZM). Fracture occurs systematically at the interface for the CO and in the coating itself for ZM, with respective fracture energies of 96.3 and 59.8 $J m^{-2}$. Finally, acoustic emission monitoring allows the detection of the damaging processes, and shows a good correlation with direct observations on broken specimens.

Acknowledgements

The authors wish to thank Mr Pouget of Renault for producing the plasma-sprayed samples and Ms Reymond of CNRS for helpful discussions about acoustic emission.

References

1. C. C. BERNDT and R. McPHERSON, *Proc. Austral. Ceram. Conf.* **9** (1980) 74.
2. M. K. FERBER and S. D. BROWN, *J. Amer. Ceram. Soc.* **64** (1981) 737.
3. P. A. SIEMERS and R. L. MEHAN, *Ceram. Eng. Sci. Proc.* **4** (1983) 828.
4. W. D. BASCOM and J. L. BITNER, *J. Mater. Sci.* **12** (1977) 1401.
5. R. F. PABST and G. ELSSNER, *ibid.* **15** (1980) 188.
6. J. WILDE, W. GROLL and F. W. KLEINLEIN, *ibid.* **20** (1985) 4069.
7. A. V. VIRKAR and R. S. GORDON, *J. Amer. Ceram. Soc.* **59** (1976) 68.
8. M. BOUSSUGE, PhD thesis, Ecole Nationale Supérieure des Mines de Paris (1985).

Received 5 June
and accepted 27 July 1987